Received: 6 August 2020 | Revised: 19 March 2022 | Accepted: 6 July 2022

DOI: 10.1002/zamm.202000207

ZAMM

ORIGINAL PAPER

Assessment of irreversibility optimization in Casson nanofluid flow with leading edge accretion or ablation

Noor Saeed Khan[1,2,3] | **Usa Wannasingha Humphries**[4] | **Wiyada Kumam**[5] | **Poom Kumam**[1,2,6] | **Taseer Muhammad**[7]

[1]KMUTTFixed Point Research Laboratory, Room SCL 802 Fixed Point Laboratory, Science Laboratory Building, Department of Mathematics, Faculty of Science, King Mongkut's University of Technology Thonburi (KMUTT), Bangkok, Thailand

[2]Center of Excellence in Theoretical and Computational Science (TaCS-CoE), Science Laboratory Building, Faculty of Science, King Mongkut's University of Technology Thonburi (KMUTT), Bangkok, Thailand

[3]Division of Science and Technology, Department of Mathematics, University of Education, Lahore, Pakistan

[4]Faculty of Science, Department of Mathematics, King Mongkut's University of Technology Thonburi (KMUTT), Bangkok, Thailand

[5]Program in Applied Statistics, Faculty of Science and Technology, Department of Mathematics and Computer Science, Rajamangala University of Technology Thanyaburi (RMUTT), Pathum Thani, Thailand

[6]Department of Medical Research, China Medical University Hospital, China Medical University, Taichung, Taiwan

[7]Department of Mathematics, College of Sciences, King Khalid University, Abha, Saudi Arabia

Correspondence
Wiyada Kumam, Program in Applied Statistics, Faculty of Science and Technology, Department of Mathematics and Computer Science, Rajamangala University of Technology Thanyaburi (RMUTT), Pathum Thani, Thailand.
Email: wiyada.kum@rmutt.ac.th

Funding information
King Khalid University, Grant/Award Number: RGP.1/248/43; Higher Education Commission, Grant/Award Number: 10534

Entropy generation in unsteady magneto-bioconvection Casson nanofluid flow with gyrotactic microorganisms in the presence of Cattaneo–Christov heat and mass flux theory is analyzed. Buongiorno nanofluid model is followed taken into account the influences of viscous dissipation, Brownian motion, and thermophoresis. Mathematica is used to compute the transformed equations through homotopy analysis method (HAM) resulting from the implementation of similarity transformations on governing equations and boundary conditions. The effects of pertinent parameters on different profiles are shown in graphs and discussed in detail.

1 | INTRODUCTION

Useless energy shows the weak performance of liquids in thermal systems. Heat transfer and friction dissipation create the irreversibility of fluids in such conditions. So, entropy generation is a hot debate for the researchers. Bejan [1] worked for the first time on entropy generation. Sahoo and Nandkeolyar [2] provided the explanatory note on entropy generation of unsteady three-dimensional MHD flow of Casson nanofluid with Brownian motion, thermophoresis, mixed convection, heat generation, viscous dissipation, and Ohmic heating using the spectral quasi-linearization method. Abbas et al. [3] considered the entropy optimized Darcy–Forchheimer electrically conducting MHD flow of the nanoparticles Molybdenum disulfide and silicon dioxide with Propylene glycol as a continuous phase fluid. Alsaadi et al. [4] examined the entropy generation in electrically conducting second grade nanofluid flow past a convectively heated surface with dissipation, Joule heating, heat source/sink, thermophoresis, and Brownian motion. Khan et al. [5] discussed the homogeneous–heterogeneous chemical reactions and entropy generation in MHD nanoparticles TiO_2-GO flow between two stretchable rotating disks subject to viscous dissipation, Joule heating, and thermal radiation. Some studies on entropy generation can be seen in the references [6–14].

In chemistry, manufacturing, non-Newtonian fluids have very important role. Alaidrous and Eid [15] investigated the mth-order reactions on the MHD flow of hyperbolic tangent nanofluid through extending surface in a porous material with thermal radiation, viscous dissipation, and Joule heating. They found that the order of the chemical reaction $m = 2$ is dominant in concentration as well as mass transfer in chemical reactions. Shehzad et al. [16] demonstrated the Casson–Maxwell fluids past stretchable rotating disk with Buongiorno nanofluid model and Cattaneo–Christov heat and mass flux theory in the presence of variable thermal conductivity. Kolsi et al. [17] analyzed the forced convection in power law nanofluid for a backward-facing flow system in the presence of double rotating cylinders with different solid volume fractions of alumina at 20 nm in diameter. Ramesh and Ojjela [18] presented the entropy generation of radiative viscoelastic second grade nanofluid in a porous channel confined between two parallel plates whose boundaries are maintained at distinct temperatures and concentrations while the fluid is being sucked and injected periodically through the upper and lower plates. Yin et al. [19] investigated the effects of nonlinear thermal radiation, variable thermal conductivity, nonuniform heat source/sink, and chemical reaction on bioconvection flow of magneto-Sisko fluid along a stretching cylinder with motile microorganisms using the Buongiorno nanofluid model. Khan et al. [20] reported the role of mixed convection and chemical reaction in Eyring Powel nanofluid using no slip condition in which a parabolic curve fitting way of communication is implemented to show the effects of Brownian motion and thermophoresis. Hayat et al. [21] studied the incompressible hyperbolic tangent liquid with convective condition using series solution. Hamid et al. [22] investigated the two-dimensional stagnation-point flow of Williamson nanofluid taking into account the effects of velocity slip, chemical reaction, and thermal radiation. Muntazir et al. [23] examined boundary layer flow of Carreau nanofluid keeping in view of magnetic dipole. They used the bvp4c technique through MATLAB-based shooting method. More studies on fluids and analytical solutions are presented in the references [24–33].

Nanofluid is a modern class of the fluid that possesses higher thermo-physical properties, that is, viscosity, thermal diffusivity, convective heat process coefficient and thermal conductivity as compare to the common traditional fluids. Therefore, nanofluids possess several industrial applications, that is, micro channel heat sources/sinks, heat exchangers, coolants and lubricants, and so forth. Ali et al. [34] examined the Stefan blowing bioconvection flow of water-based nanofluid with Cattaneo–Christov heat and mass flux theory by implementing the finite element method. Vasu et al. [35] investigated the MHD bioconvection nanofluid flow of Casson thin film with uniform thickness using the Buongiorno nanofluid model. Jiang et al. [36] studied the Stefan blowing effect on hybrid nanfluid in connection with Cattaneo–Christov heat and mass flux theory as well as gyrotactic microorganisms through bvp4c approach. Ali et al. [37] inspected a mathematical model of MHD nanofluid flow considering Cattaneo–Christov heat flux in which Cattaneo–Christov heat flux model has proved the enhanced results. Ilias et al. [38] worked on the unsteady aligned MHD boundary layer nanofluid flow with water and kerosene based fluids and Fe_3O_4 as well as Al_2O_3 nanoparticles. Zeeshan et al. [39] applied the homotopy analysis method (HAM) to evaluate the solution of a problem of thin film nanofluid in three dimensions past a stretchable inclined surface. Goqo et al. [40] implemented the bivariate spectral quasi-linearization technique to study the nanofluid flow past a non-isothermal wedge. Hosseinzadeh et al. [41] examined the ethylene glycol-based carbon nanotubes with thermal radiation, porosity, and entropy generation. The references [42–57] provide few other studies on nanofluid subject.

The present study furnishes the development of Cattaneo–Christov heat and mass flux model of leading edge accretion or ablation with entropy generation in bioconvection Casson nanofluid flow. The series solution is found through analytical technique HAM [58–66].

2 | MATHEMATICAL FORMULATION

An incompressible time-dependent bioconvection Casson nanofluid flow is investigated with Cattaneo–Christov heat and mass flux in the presence of entropy generation. Magnetic field B is applied perpendicularly to the flow. The physical form is shown in Figure 1.

The problem has the following governing equations for Casson nanofluid as in Refs. [34–37]

$$\frac{\partial u}{\partial x} + \frac{\partial v}{\partial y} = 0, \tag{1}$$

$$\frac{\partial u}{\partial t} + u\frac{\partial u}{\partial x} + v\frac{\partial u}{\partial y} = U_\infty \frac{\partial U_\infty}{\partial x} + \frac{\partial U_\infty}{\partial t} + \frac{\mu_f}{\rho_f}\left(1 + \frac{1}{\beta}\right)\frac{\partial^2 u}{\partial y^2} - \frac{\sigma_f B_0^2 u}{\rho_f}, \tag{2}$$

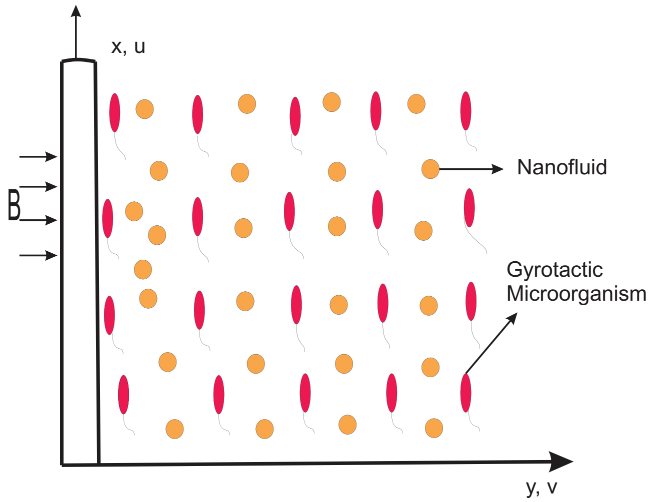

FIGURE 1 Mechanism of the problem

$$\frac{\partial T}{\partial t}+u\frac{\partial T}{\partial x}+v\frac{\partial T}{\partial y}=\frac{\partial^2 T}{\partial y^2}\frac{k_f}{(\rho c_P)_f}+\frac{\mu_f}{(\rho c_P)_f}\left[\frac{\partial u}{\partial y}\right]^2+\frac{\sigma_f B_0^2 u}{\rho_f}-2\gamma_1\left[u\frac{\partial^2 T}{\partial t\partial x}+v\frac{\partial^2 T}{\partial t\partial y}+uv\frac{\partial^2 T}{\partial x\partial y}\right]$$
$$-\gamma_1\left[\frac{\partial^2 T}{\partial t^2}+\frac{\partial u}{\partial t}\frac{\partial T}{\partial x}+\frac{\partial v}{\partial t}\frac{\partial T}{\partial y}+u^2\frac{\partial^2 T}{\partial x^2}+\left[u\frac{\partial v}{\partial x}+v\frac{\partial v}{\partial y}\right]\frac{\partial T}{\partial y}+v^2\frac{\partial^2 T}{\partial y^2}+\left[v\frac{\partial u}{\partial y}+u\frac{\partial u}{\partial x}\right]\frac{\partial T}{\partial x}\right]-\frac{\partial q_r}{\partial y}$$
$$+\tau\left[D_B\frac{\partial T}{\partial y}\frac{\partial C}{\partial y}+\frac{D_T}{T_\infty}\left(\frac{\partial T}{\partial y}\right)^2\right], \tag{3}$$

$$\frac{\partial C}{\partial t}+u\frac{\partial C}{\partial x}+v\frac{\partial C}{\partial y}+\gamma_2\left[\frac{\partial^2 C}{\partial t^2}+\frac{\partial u}{\partial t}\frac{\partial C}{\partial x}+\frac{\partial v}{\partial t}\frac{\partial C}{\partial y}+u^2\frac{\partial^2 C}{\partial x^2}+v^2\frac{\partial^2 C}{\partial x^2}\right]=D_B\frac{\partial^2 C}{\partial y^2}+\frac{D_T}{T_\infty}\frac{\partial^2 T}{\partial y^2}$$
$$-2\gamma_2\left[u\frac{\partial^2 C}{\partial t\partial x}+v\frac{\partial^2 C}{\partial t\partial y}+uv\frac{\partial^2 C}{\partial x\partial y}\right]-\gamma_2\left[u\frac{\partial v}{\partial x}+v\frac{\partial v}{\partial y}\right]\frac{\partial C}{\partial y}-\gamma_2\left[v\frac{\partial u}{\partial y}+u\frac{\partial u}{\partial x}\right]\frac{\partial C}{\partial x}, \tag{4}$$

$$\frac{\partial N}{\partial t}+u\frac{\partial N}{\partial x}+v\frac{\partial N}{\partial y}+\frac{bW_c}{(C_w-C_\infty)}\frac{\partial}{\partial y}\left(N\frac{\partial C}{\partial y}\right)=D_m\frac{\partial^2 N}{\partial y^2}, \tag{5}$$

with boundary conditions used as [34–37]

$$u=u_w=\lambda U_\infty,\quad v=-\frac{D_m}{1-C_w}\frac{\partial C}{\partial y},\quad N=N_w,\quad T=T_w,\quad C=C_w,\quad at\quad y=0, \tag{6}$$

$$u=u_e=U_\infty,\quad N\to N_\infty,\quad T\to T_\infty,\ C\to C_\infty,\ as\quad y\to\infty, \tag{7}$$

where u, v are the velocity components in x, y directions. U_∞ is the free stream velocity, β is the Casson fluid parameter, γ_1 is the thermal relaxation time parameter, γ_2 is the concentration time relaxation parameter. D_T, D_B, D_m are the thermophoretic diffusion, Brownian diffusion, and gyrotactic microorganisms diffusion coefficient, respectively. σ_f is the electrical conductivity and $\tau=\frac{(\rho c)_P}{(\rho c)_f}$ is the ratio of heat capacity of nanoparticles to heat capacity of nanofluid. b is the chemotaxis constant and W_c is the maximum cell swimming speed. The subscript f denotes the nanofluid while μ_f, ρ_f, k_f, and $(\rho c_P)_f$ are, respectively, the dynamic viscosity, density, thermal conductivity, and heat capacity of Casson nanofluid. u_e is the external velocity and λ is used for stretching/shrinking parameter. (T_w, C_w, N_w) and $(T_\infty, C_\infty, N_\infty)$ are the Casson nanofluid temperature, nanoparticles concentration, gyrotactic microorganisms concentration at surface and infinity, respectively. q_r is the radiative heat flux and is defined through Rosseland approximation [26] as

$$q_r=-\frac{4\sigma_1}{3k_1}\frac{\partial T^4}{\partial y}, \tag{8}$$

where σ_1 and k_1 are the Stefan–Boltzmann constant and the mean absorption coefficient, respectively. Assuming that the differences in temperature within the flow are such that T^4 can be written as a linear combination of the temperature and through the Taylor's theorem about T_∞ and neglecting the higher order terms, it provides

$$T^4 = 4T_\infty^3 T - 3T_\infty^4. \tag{9}$$

So

$$\frac{\partial q_r}{\partial y} = -\frac{16T_\infty^3\sigma_1}{3k_1}\frac{\partial^2 T}{\partial y^2}. \tag{10}$$

Introducing the similarity transformations for f, ζ, θ, ϕ, and χ as the nondimensional quantities of velocity, variable, temperature, nanoparticles concentration, and gyrotactic microorganisms concentration, respectively, as

$$\psi(x,y,t) = U_\infty\sqrt{\nu_f t\cos\gamma + (\nu_f x/U_\infty)\sin\gamma}\, f(\zeta),\ \frac{\partial\psi}{\partial y} = u,\ -\frac{\partial\psi}{\partial x} = v,$$
$$\zeta = y/\sqrt{\nu_f t\cos\gamma + (\nu_f x/U_\infty)\sin\gamma},\quad \theta(\zeta) = \frac{T - T_\infty}{T_w - T_\infty},\quad \phi(\zeta) = \frac{C - C_\infty}{C_w - C_\infty},\quad \chi(\zeta) = \frac{N - N_\infty}{N_w - N_\infty}, \tag{11}$$

where ψ is the stream function. ν_f is used for the kinematic viscosity. γ is the leading edge accretion/ablation parameter where $(t\cos\gamma\nu_f + \sin\gamma(\nu_f x/U_\infty))$ must be higher than zero [34, 36].

The continuity Equation (1) is satisfied through Equation (11).

Using Equation (11), the governing Equations (2–7) are simplified to the following equations:

$$\left(1+\frac{1}{\beta}\right)f''' + \frac{1}{2}\zeta f''(\cos\gamma) + \frac{1}{2}ff''(\sin\gamma) - Mf' = 0, \tag{12}$$

$$\frac{(1+Rd)}{Pr}\theta'' + \frac{1}{2}\left[\left(f(\sin\gamma) + \zeta(\cos\gamma)\right)\theta' + \gamma_3\sin\gamma\left(3ff'\theta' + \zeta f\theta''\right)\right] + Ecf''^2 + Mf'^2 + Nb\theta'\phi' + Nt\theta'^2 = 0, \tag{13}$$

$$\phi'' + \frac{1}{2}PrLe\left[\left(f(\sin\gamma) + \zeta(\cos\gamma)\right)\phi' + \gamma_4\sin\gamma\left(3ff'\phi' + \zeta f\phi''\right)\right] + \frac{Nt}{Nb}\theta'' = 0, \tag{14}$$

$$\chi'' + \frac{1}{2}PrLb\left[\left(f(\sin\gamma) + \zeta(\cos\gamma)\right)\chi'\right] - Pe\left(\chi\phi'' + \chi'\phi'\right) = 0, \tag{15}$$

$$f = \frac{2}{LePr}\frac{1}{\sin\gamma}f_w\phi',\quad f' = \lambda,\quad \theta = 1,\quad \phi = 1,\quad \chi = 1,\quad at\quad \zeta = 0, \tag{16}$$

$$f' = 1,\quad \theta = 0,\quad \phi = 0,\quad \chi = 0,\quad at\quad \zeta = \infty, \tag{17}$$

where ($'$) is the derivative with respect to ζ. $M = \dfrac{2\left(\nu_f t\cos\gamma + (\nu_f x/U_\infty)\sin\gamma\right)\sigma_f B_0^2}{\mu_f}$ is the magnetic field parameter, $Nt = \dfrac{\tau D_T(T_w - T_\infty)}{k_f T_\infty}$ is the thermophoresis parameter, $Nb = \dfrac{\tau D_B(C_w - C_\infty)}{k_f}$ is the Brownian motion parameter, $Pe = \dfrac{bW_c}{D_m}$ is the bioconvection Peclet number. $Pr = \dfrac{\nu_f}{k_f}$, $Ec = \dfrac{(U_\infty)^2}{(c_P)_f(T_w - T_\infty)}$, $Le = \dfrac{\nu_f}{D_B}$, $Lb = \dfrac{\nu_f}{D_m}$, and $f_w = \dfrac{C_w - C_\infty}{1 - C_\infty}$ are the Prandtl, Eckert, Lewis, bioconvection Lewis numbers, and suction/injection parameter, respectively. Also, $\gamma_3 = \gamma_1 U_\infty, \gamma_4 = \gamma_2 U_\infty$, and $Rd = \dfrac{16T_1^3\sigma_1}{3k_1k_f}$ are the nondimensional thermal relaxation, solutal relaxation, and thermal radiation parameters, respectively.

When the Casson parameter β tends to ∞, the fluid turns into a Newtonian fluid. For, $\gamma_3 = 0$ and $\gamma_3 = 0$, the classical Fourier's law and Fick model are recovered.

3 | ENTROPY GENERATION

An equation representing the entropy generation [12] is

$$E'''_{gen} = \left[\frac{\partial T}{\partial y}\right]^2 \frac{k_f}{T_\infty^2} + \frac{k_f}{T_\infty^2}\left[\frac{16\sigma_1 T_\infty^3}{3k_1}\right]\left(\frac{\partial T}{\partial y}\right)^2 + \frac{\mu_f}{T_\infty}\left(1+\frac{1}{\beta}\right)\left(\frac{\partial u}{\partial y}\right)^2 + \left[\frac{\partial u}{\partial y}\right]^2 \frac{\mu_f}{T_\infty} + \left[\frac{\partial C}{\partial y}\right]^2 \frac{RD}{C_\infty}$$
$$+ \left[\frac{\partial C}{\partial x}\frac{\partial T}{\partial x} + \frac{\partial C}{\partial y}\frac{\partial T}{\partial y}\right]\frac{RD}{T_\infty} + \left[\frac{\partial N}{\partial y}\right]^2 \frac{RD}{N_\infty} + \left[\frac{\partial N}{\partial x}\frac{\partial T}{\partial x} + \frac{\partial N}{\partial y}\frac{\partial T}{\partial y}\right]\frac{RD}{T_\infty} + \frac{\sigma_f B_0^2 u^2}{T_\infty}, \tag{18}$$

where R is the ideal gas constant while D is the diffusivity.

The characteristic entropy generation rate is

$$E_0''' = \frac{k_f (T_w - T_\infty)^2}{T_\infty^2}. \tag{19}$$

The nondimensional entropy generation $N_G(\zeta)$ is obtained with the help of Equation (11) as

$$N_G(\zeta) = \frac{E'''_{gen}}{E_0'''}. \tag{20}$$

So

$$N_G(\zeta) = Re\left[1+\frac{4}{3}Rd\right]\theta'^2 + \frac{ReBr}{(\theta_w)^2}\left[f''^2 + Mf'^2\right] + \frac{ReBr}{(\theta_w)^2}\left(1+\frac{1}{\beta}\right)f'^2 + Re\gamma_5\left[\frac{\phi_w}{\theta_w}\right]^2\phi'^2$$
$$+Re\gamma_5\left[\frac{\phi_w}{\theta_w}\right]\theta'\phi' + Re\gamma_6\left[\frac{\chi_w}{\theta_w}\right]^2\chi'^2 + Re\gamma_6\left[\frac{\chi_w}{\theta_w}\right]\theta'\chi', \tag{21}$$

where $Re = \dfrac{x^2}{\nu_f t\cos\gamma + (\nu_f x/U_\infty)\sin\gamma}$ is the Reynolds number, $\theta_w = \dfrac{T_w - T_\infty}{T_\infty}$ is the temperature difference parameter, $Br = \dfrac{\mu_f U_\infty^2}{k_f T_\infty}$ is the Brinkman number, $\gamma_5 = \dfrac{RDC_\infty}{k_f}$ is the diffusion constant parameter due to nanoparticles concentration, $\gamma_6 = \dfrac{RDN_\infty}{k_f}$ is the diffusion constant parameter due to gyrotactic microorganisms concentration, $\phi_w = \dfrac{C_w - C_\infty}{C_\infty}$ is the nanoparticles concentration difference parameter, and $\chi_w = \dfrac{N_w - N\infty}{N_\infty}$ is the gyrotactic microorganisms concentration difference parameter.

4 | SOLUTION OF THE PROBLEM

Implementing HAM [58], choosing the initial approximations as

$$f_0(\zeta) = \frac{\exp(-\zeta)(LePr - \exp(\zeta)LePr + \exp(\zeta)LePr\zeta) - \lambda LePr + \lambda\exp(\zeta)LePr\zeta) - 2\exp(\zeta)f_w\cos\gamma}{LePr},$$
$$\theta_0(\zeta) = \exp(-\zeta),\ \phi_0(\zeta) = \exp(-\zeta),\ \chi_0(\zeta) = \exp(-\zeta). \tag{22}$$

Now by following HAM, the zeroth and mth order deformation problems [58] are evaluated and hence the solution.

5 | RESULTS AND DISCUSSION

HAM [58] is used to solve the nondimensional equations. Figure 2 depicts the influence of Casson nanofluid parameter β on velocity $f'(\zeta)$. It is seen that the rising values of Casson nanofluid parameter leads to increase the velocity $f'(\zeta)$.

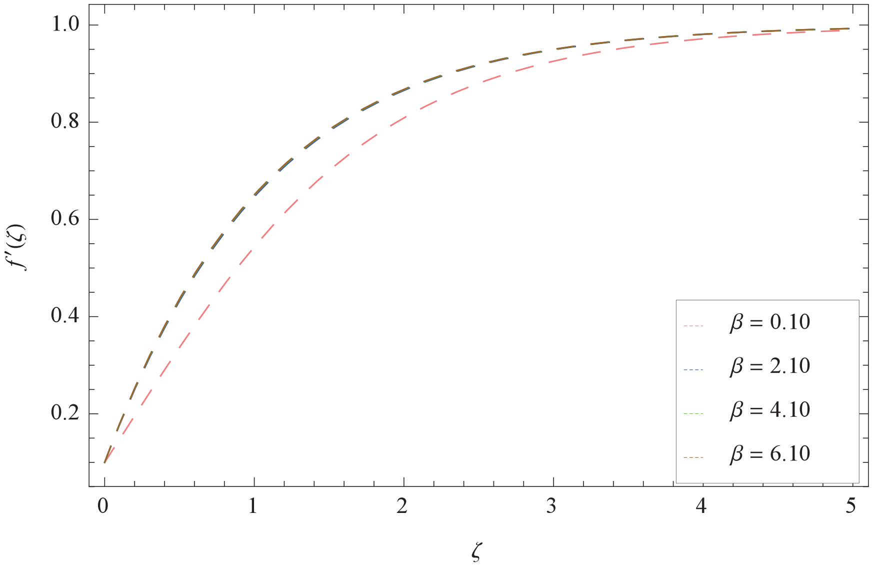

FIGURE 2 Influence of Casson nanofluid parameter β on velocity $f'(\zeta)$

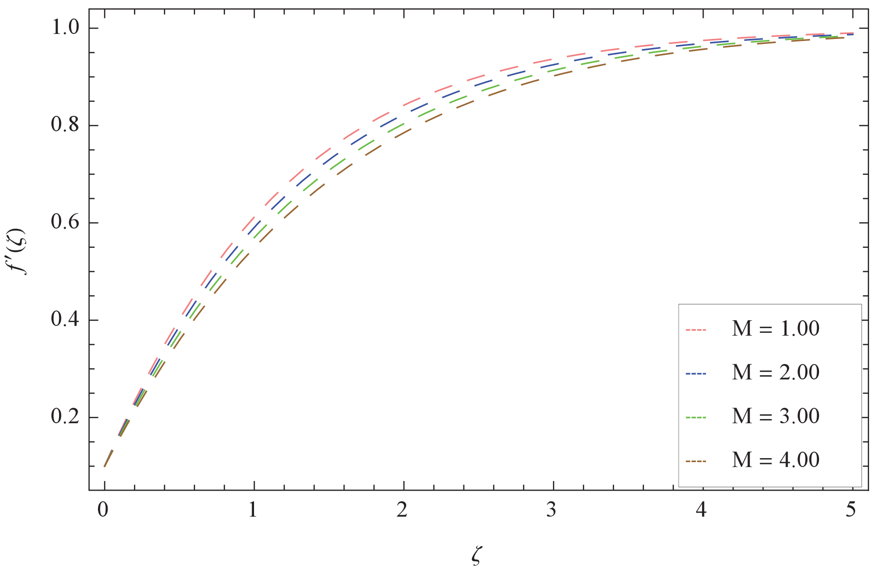

FIGURE 3 Influence of magnetic field parameter M on velocity $f'(\zeta)$

Figure 3 demonstrates that due to the increasing values of magnetic field parameter M, the Casson nanofluid motion retards. The existence of magnetic field creates a resistive force, called the Lorentz force, which is responsible for the resistivity of flow of Casson nanofluid. The effect of suction/injection or Stefan blowing parameter f_w on velocity $f'(\zeta)$ in Figure 4 shows that the boundary layer gets thinning. The buoyancy forces decelerate the nanofluid flow. From Figure 5, it is observed that stretching/shrinking parameter λ has influenciable role in the dynamic of present system. The velocity $f'(\zeta)$ increases for the stretching case, that is, for $\lambda = 0.10, 0.20, 0.30, 0.40$.

Figure 6 shows that the magnetic field parameter M has the characteristic to boost the Ohmic heating and hence the Casson nanofluid temperature $\theta(\zeta)$ within boundary layer. The decreasing behavior of heat transfer $\theta(\zeta)$ due to the effect of Prandtl number Pr is observed in Figure 7. It is noted in Figure 8 that on account of high values of thermal radiation parameter Rd, the temperature $\theta(\zeta)$ is high. Figure 9 reveals that heat transfer $\theta(\zeta)$ is intensified through the greater values of Stefan blowing parameter f_w. The nanofluid addition via boundary energizes species diffusion in the system so the heat transfer is enhanced. Figure 10 displays the effect of Eckert number Ec on temperature distribution. The reason is that nanofluid particles collide more frequently as a result, the temperature rises. It is indicated by Figure 11 that heat transfer $\theta(\zeta)$ is increased with the thermophoresis parameter Nt. The thermophoretic phenomena supports the heat expansion in the system. The enhanced values of Brownian motion parameter Nb cause rise in the temperature as plotted in Figure 12. Physically, through nanoparticles injection, the thermal conduction is improved. Figure 13 exhibits

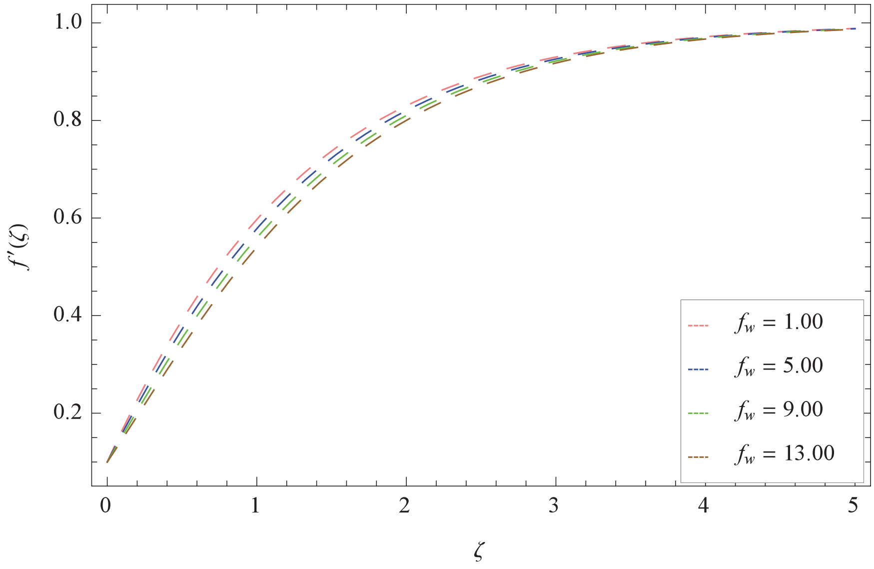

FIGURE 4 Influence of suction/injection parameter f_w on velocity $f'(\zeta)$

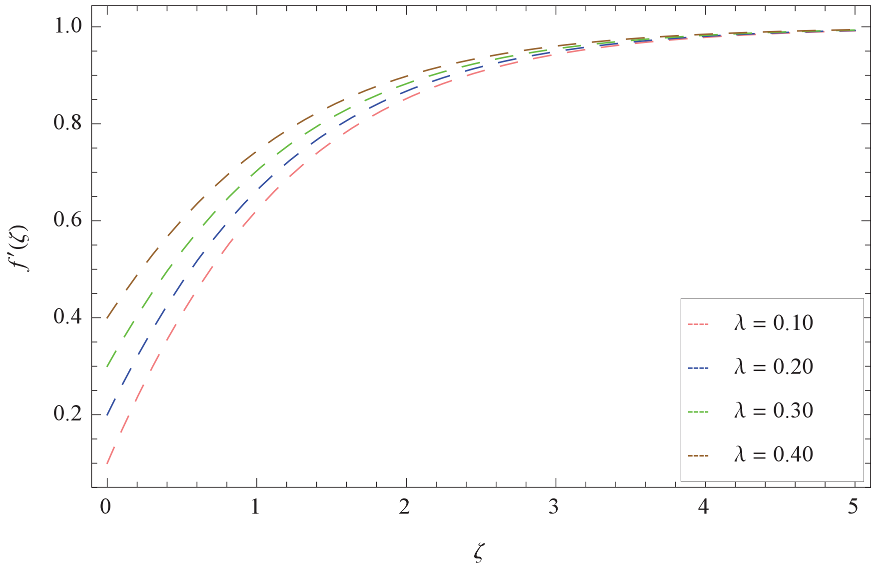

FIGURE 5 Influence of stretching/shrinking parameter λ on velocity $f'(\zeta)$

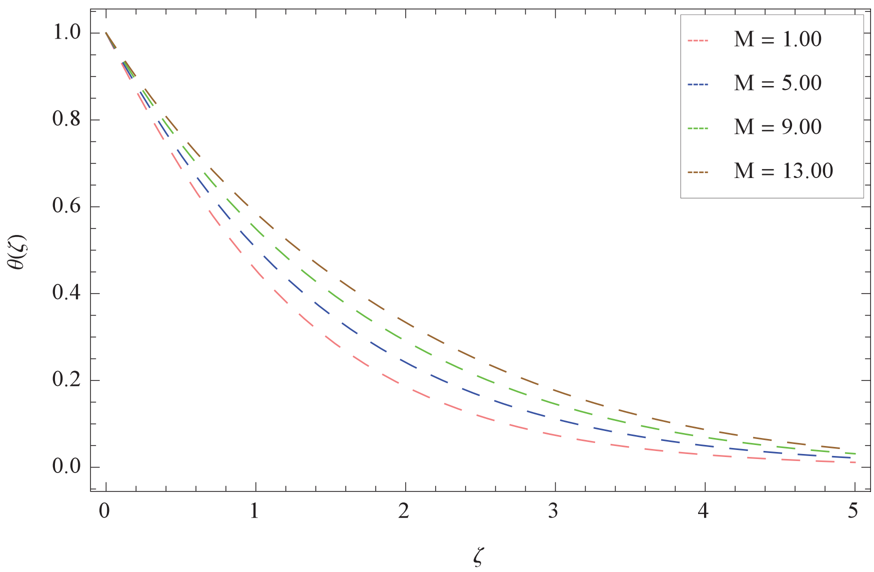

FIGURE 6 Influence of magnetic field parameter M on heat transfer $\theta(\zeta)$

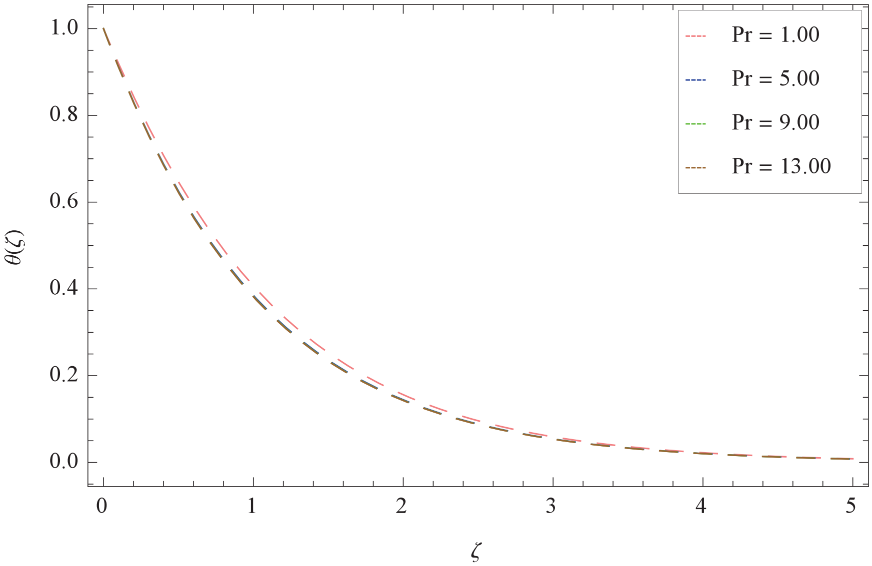

FIGURE 7 Influence of Prandtl number Pr on heat transfer $\theta(\zeta)$

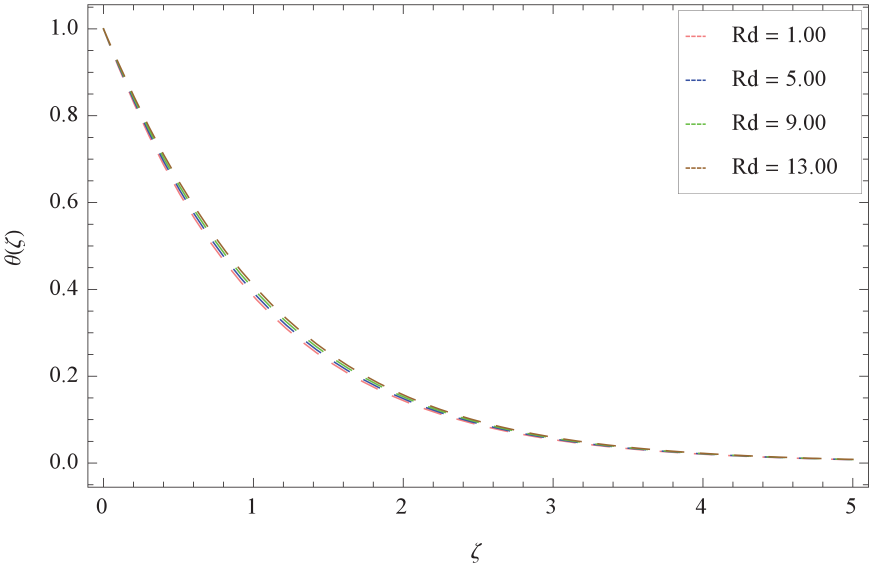

FIGURE 8 Influence of thermal radiation parameter Rd on heat transfer $\theta(\zeta)$

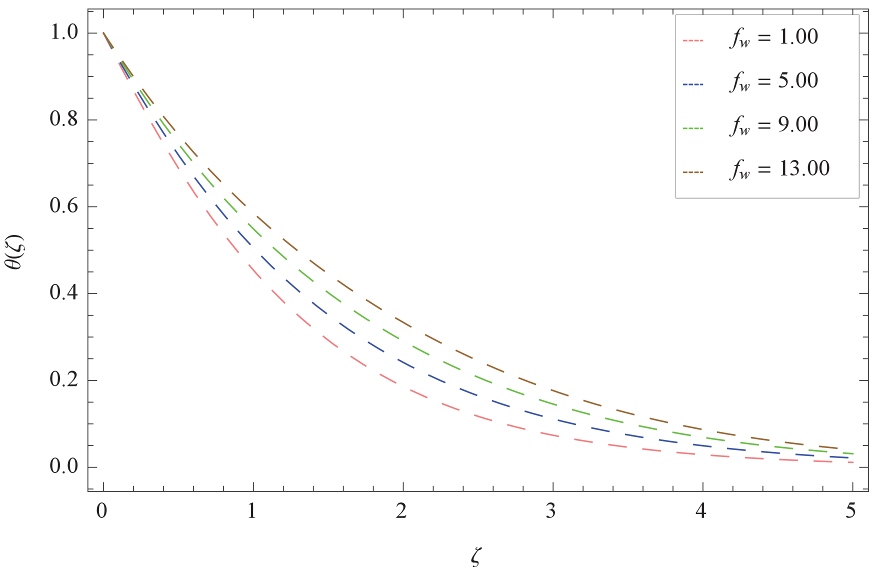

FIGURE 9 Influence of suction/injection parameter f_w on heat transfer $\theta(\zeta)$

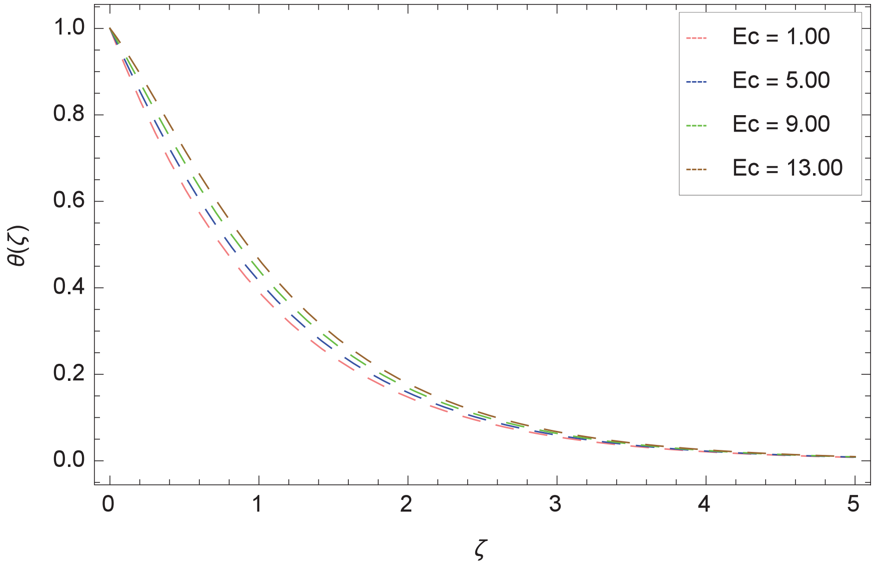

FIGURE 10 Influence of Eckert number Ec on heat transfer $\theta(\zeta)$

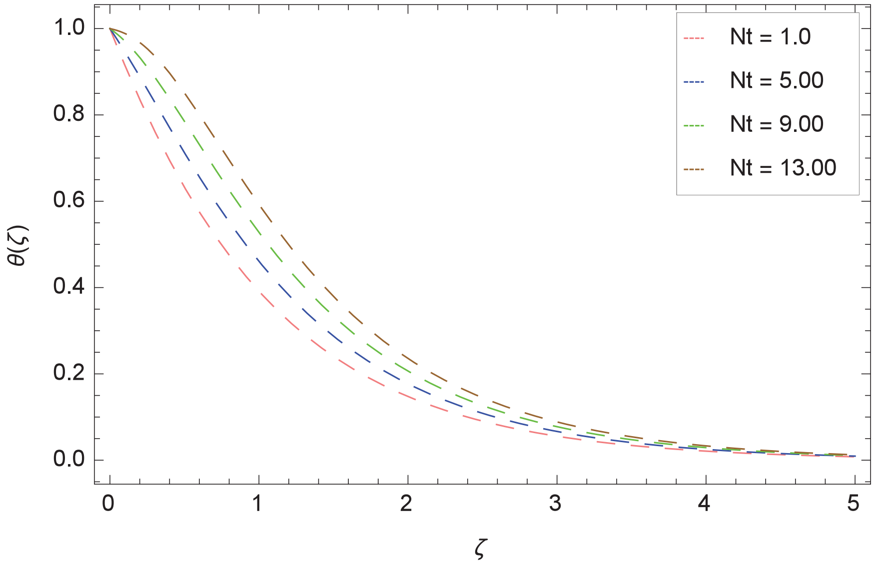

FIGURE 11 Influence of thermophoresis parameter Nt on heat transfer $\theta(\zeta)$

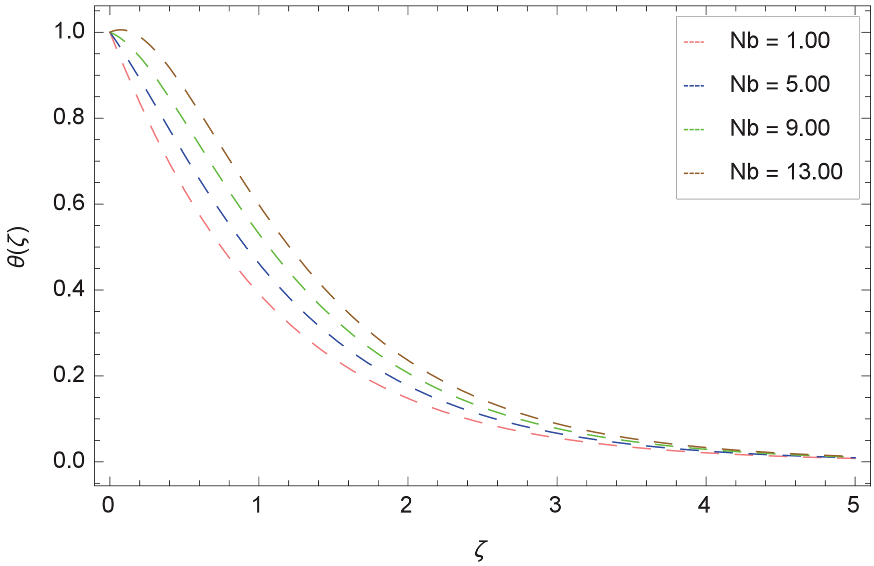

FIGURE 12 Influence of Brownian motion parameter Nb on heat transfer $\theta(\zeta)$

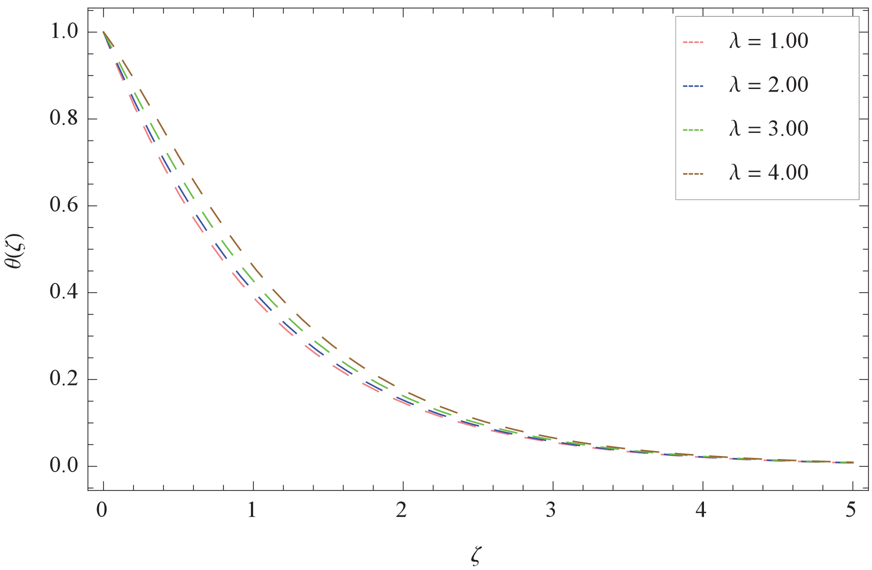

FIGURE 13 Influence of stretching/shrinking parameter λ on heat transfer $\theta(\zeta)$

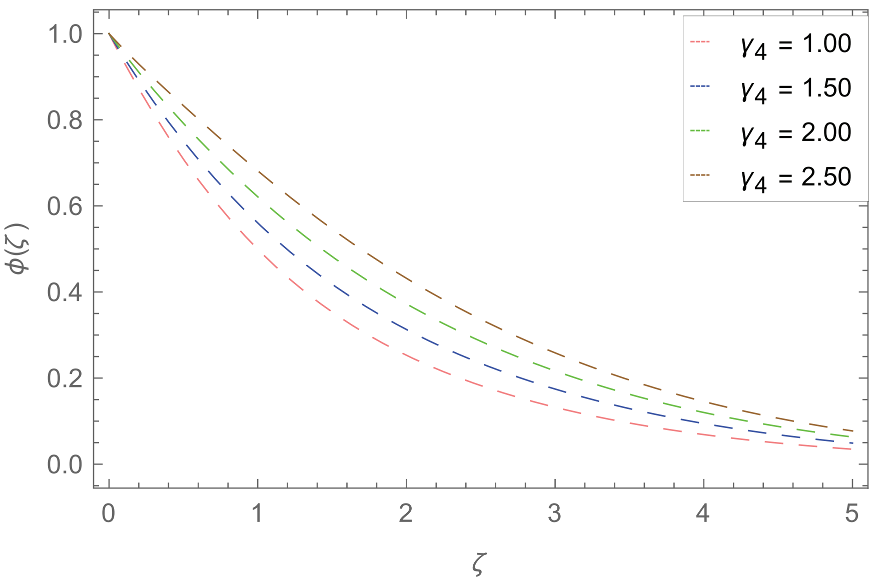

FIGURE 14 Influence of solutal relaxation parameter γ_4 on nanoparticles concentration $\phi(\zeta)$

that stretching/shrinking parameter λ increases the temperature profile $\theta(\zeta)$. The present case shows the investigations on stretching case for the values $\lambda = 1.00, 2.00, 3.00, 4.00$.

Figure 14 shows the behavior of solutal relaxation parameter γ_4 and nanoparticles concentration profile $\phi(\zeta)$. The nanoparticles concentration is increased since due to the effect of γ_4, less time is consumed in transporting the nanoparticles from one place to another one. The influence of Lewis number Le on nanoparticles concentration profile $\phi(\zeta)$ is elaborated in Figure 15. Since Le is related to thermal diffusivity to mass diffusivity so by the greater values of Le, nanoparticles concentration profile $\phi(\zeta)$ is reduced initially and then increases gradually. The effect of suction/injection or Stefan blowing parameter f_w on nanoparticles concentration profile $\phi(\zeta)$ is shown in Figure 16. The injection of nanoparticles to the Casson fluid provides more diffusion and so the $\phi(\zeta)$ is enhanced. Figure 17 is sketched to show the role of Brownian motion parameter Nb and nanoparticles concentration $\phi(\zeta)$. Due to the Brownian motion of nanoparticles, the concentration is reduced. The effect of thermophoresis parameter Nt in Figure 18 represents that $\phi(\zeta)$ is enhanced for the various values of Nt. Through the stretching values of λ, the nanoparticles concentration $\phi(\zeta)$ is minimum as shown by Figure 19.

The decreasing effects of Lewis and bioconvection Lewis numbers for gyrotactic microorganisms concentration $\chi(\zeta)$ are, respectively, shown in Figures 20 and 21. The higher estimates of bioconvection Peclet number also reduce the gyrotactic microorganisms concentration $\chi(\zeta)$ as shown in Figure 22. The larger values of suction/injection or Stefan blowing parameter f_w indicate in Figure 23 that gyrotactic microorganisms concentration $\chi(\zeta)$ is increased as more space is generated

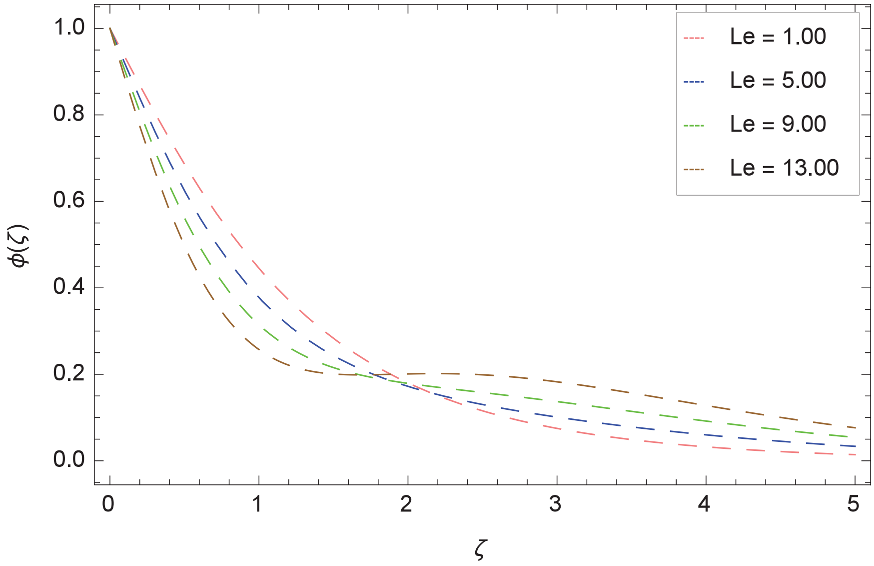

FIGURE 15 Influence of Lewis number *Le* on nanoparticles concentration $\phi(\zeta)$

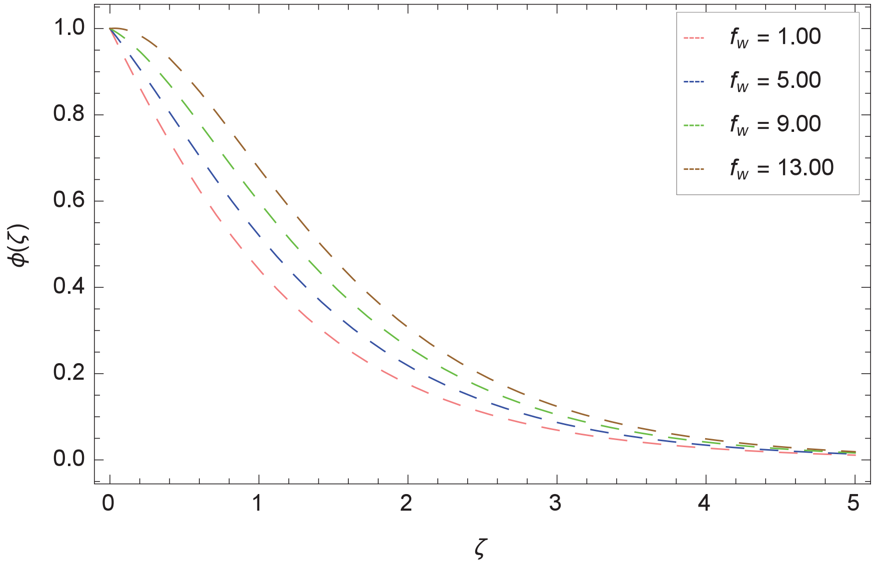

FIGURE 16 Influence of suction/injection parameter f_w on nanoparticles concentration $\phi(\zeta)$

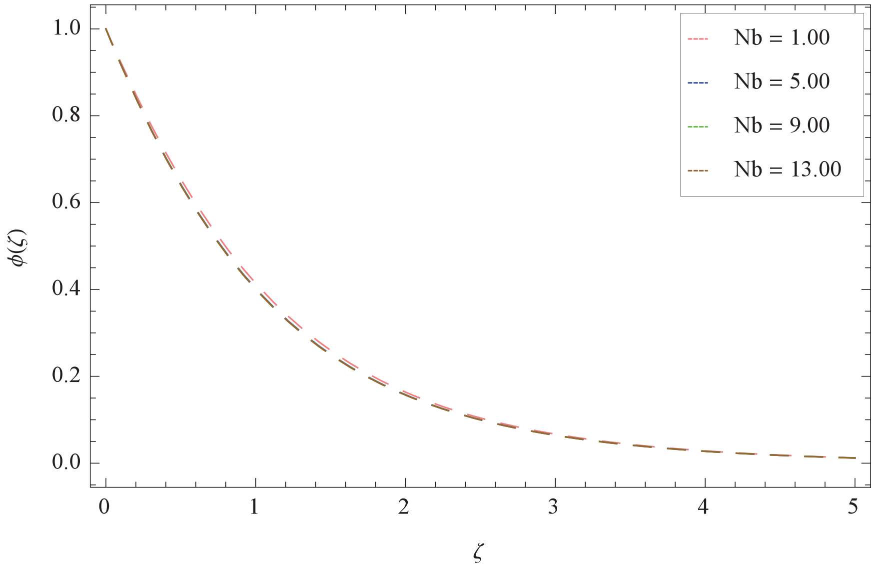

FIGURE 17 Influence of Brownian motion parameter *Nb* on nanoparticles concentration $\phi(\zeta)$

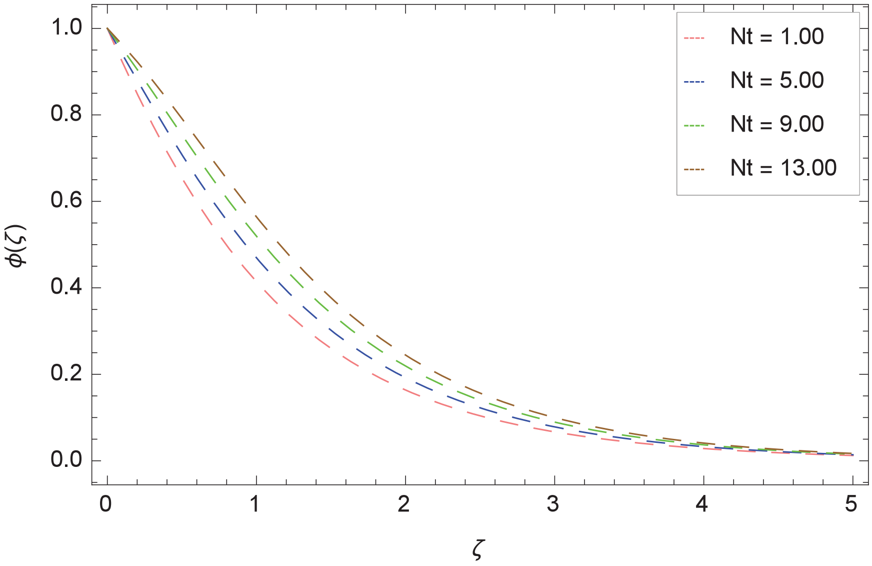

FIGURE 18 Influence of thermophoresis parameter Nt on nanoparticles concentration $\phi(\zeta)$

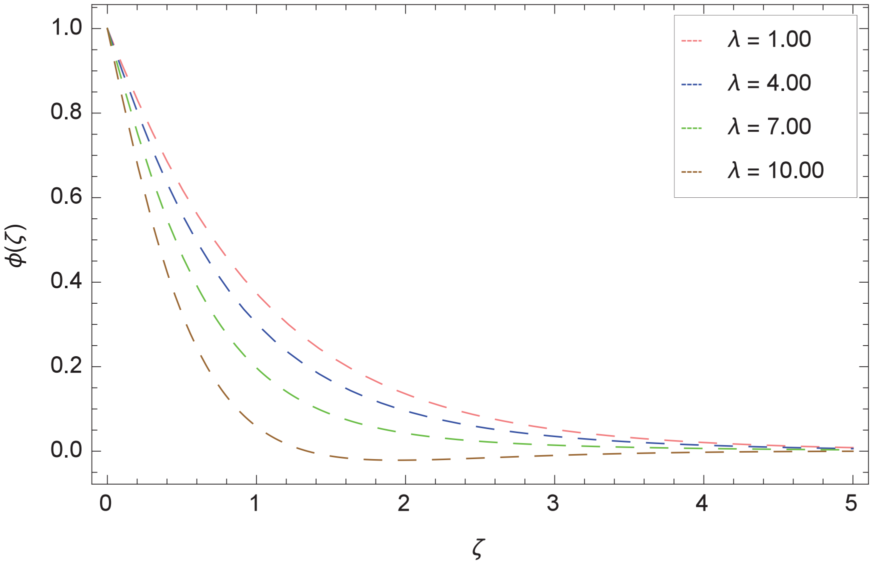

FIGURE 19 Influence of stretching/shrinking parameter λ on nanoparticles concentration $\phi(\zeta)$

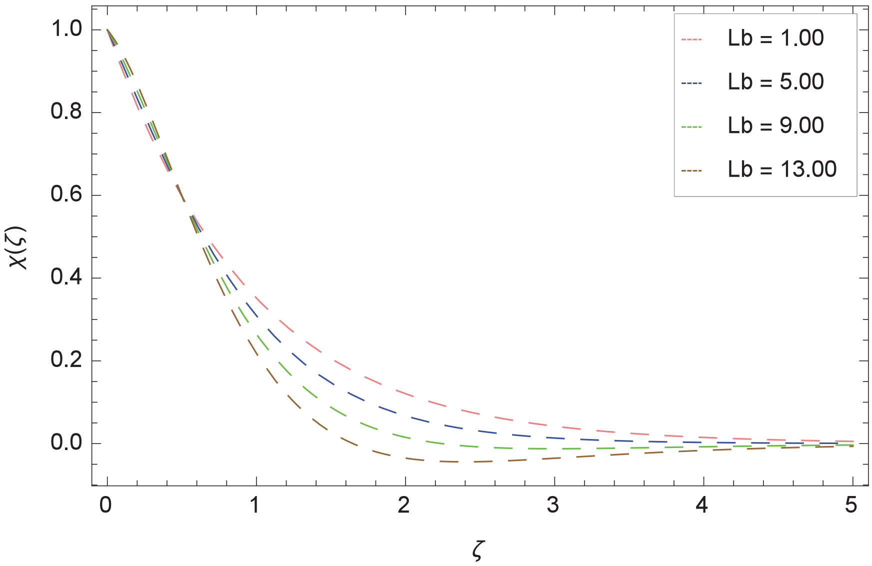

FIGURE 20 Influence of bioconvection Lewis number Lb on gyrotactic microorganisms concentration $\chi(\zeta)$

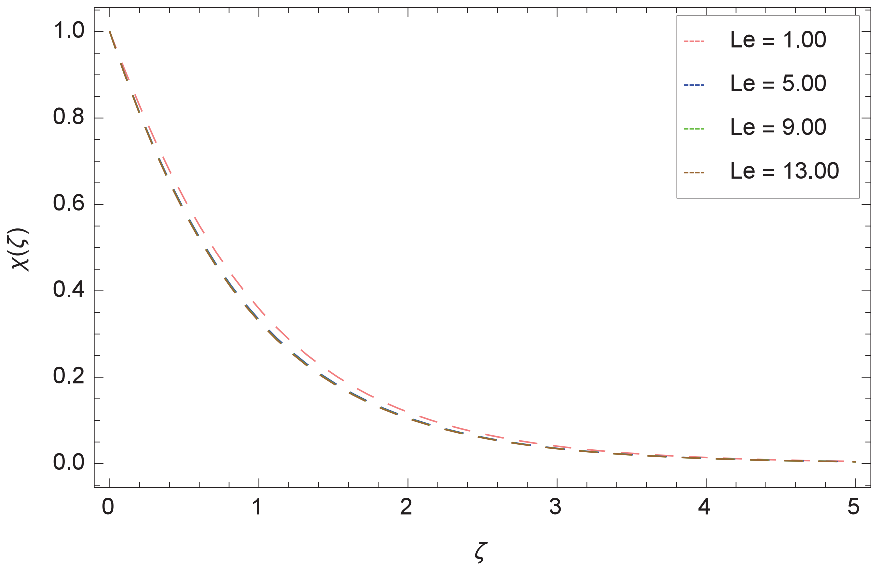

FIGURE 21 Influence of Lewis number *Le* on gyrotactic microorganisms concentration $\chi(\zeta)$

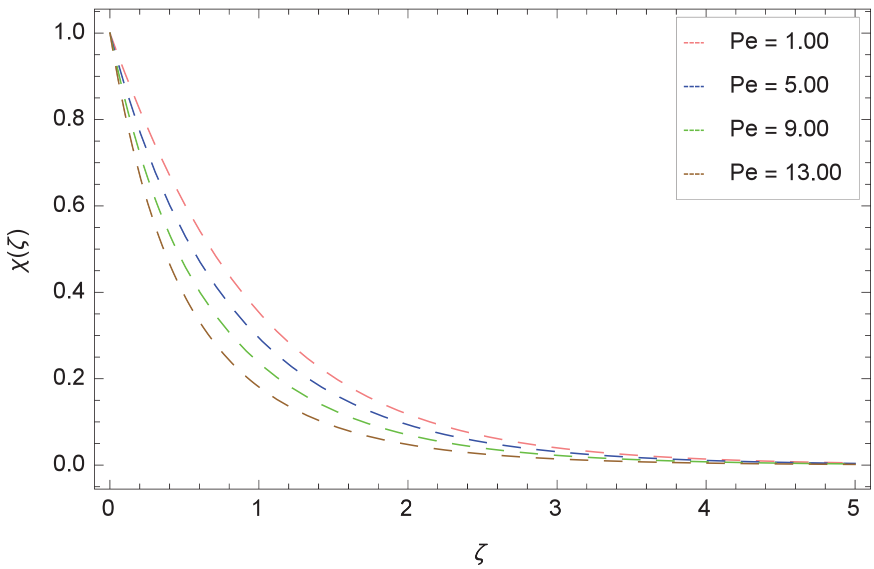

FIGURE 22 Influence of bioconvection Peclet number *Pe* on gyrotactic microorganisms concentration $\chi(\zeta)$

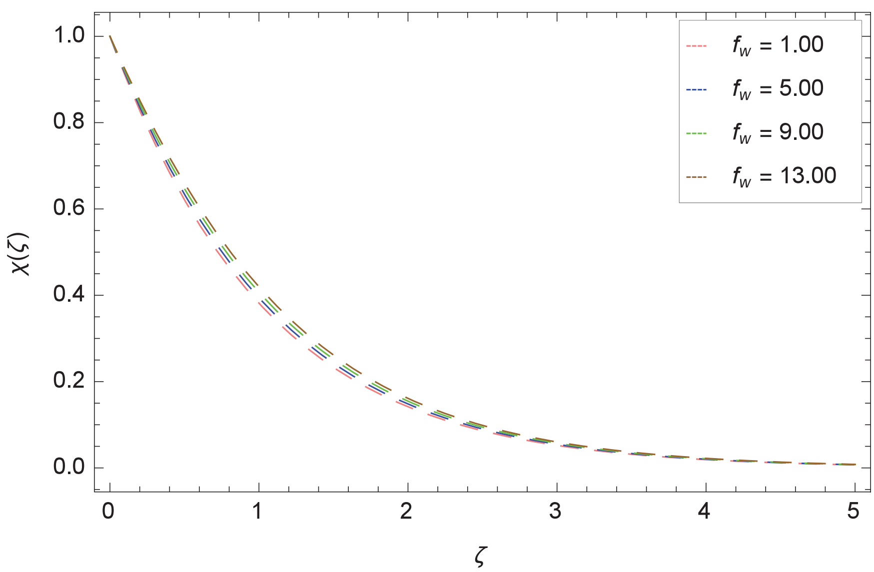

FIGURE 23 Influence of suction/injection parameter f_w on gyrotactic microorganisms concentration $\chi(\zeta)$

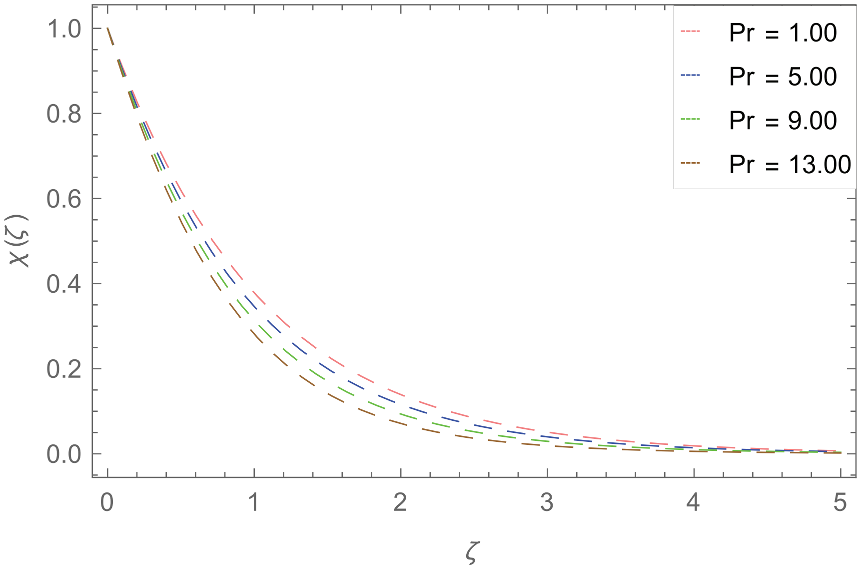

FIGURE 24 Influence of Prandtl number Pr on gyrotactic microorganisms concentration $\chi(\zeta)$

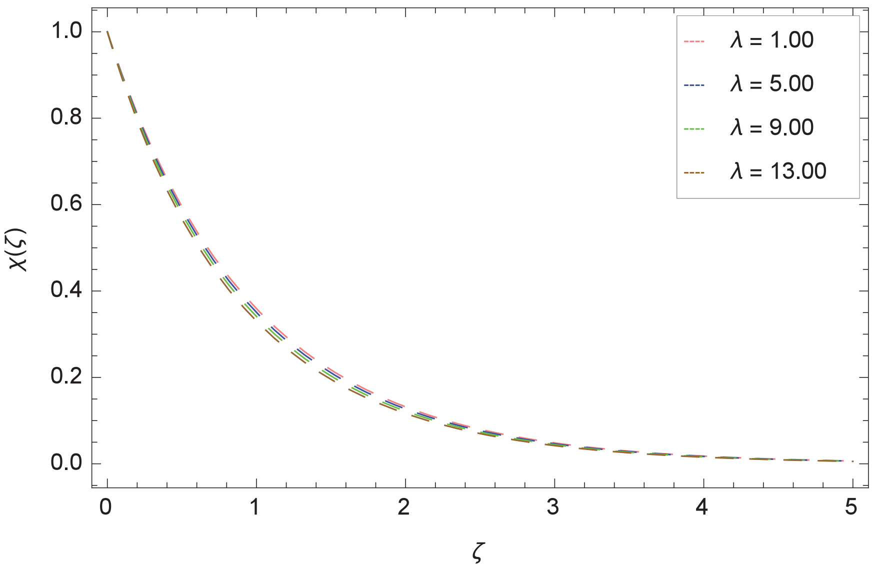

FIGURE 25 Influence of stretching/shrinking parameter λ on gyrotactic microorganisms concentration $\chi(\zeta)$

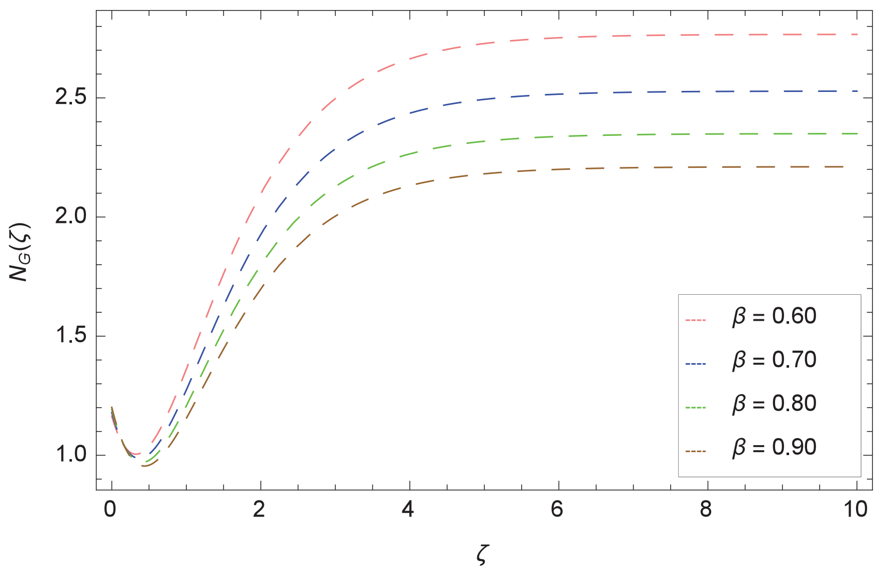

FIGURE 26 Influence of Casson nanofluid parameter β on entropy generation rate $N_G(\zeta)$

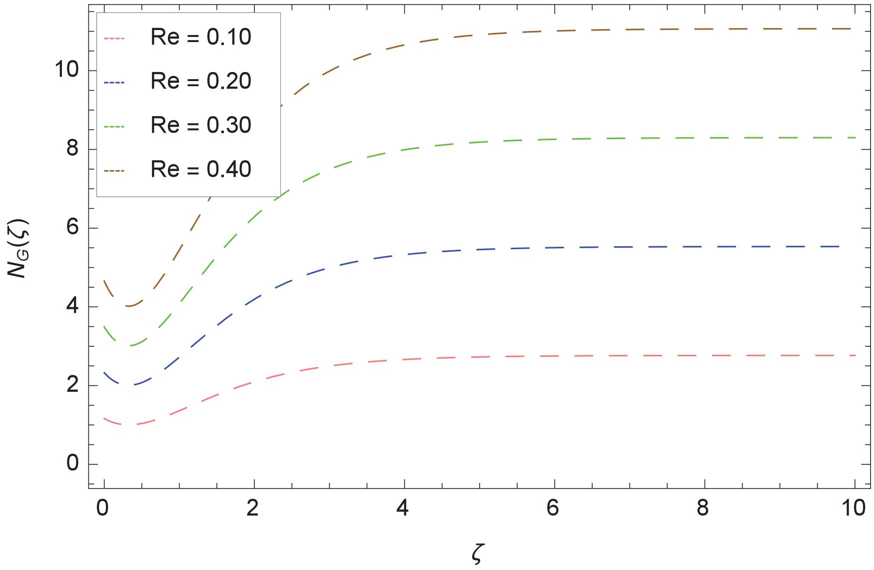

FIGURE 27 Influence of Reynolds number Re on entropy generation rate $N_G(\zeta)$

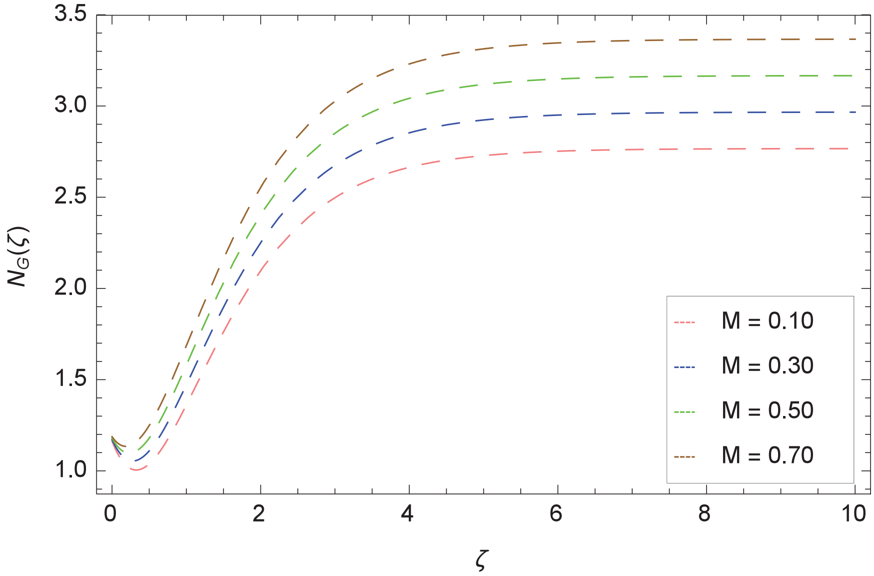

FIGURE 28 Influence of magnetic field parameter M on entropy generation rate $N_G(\zeta)$

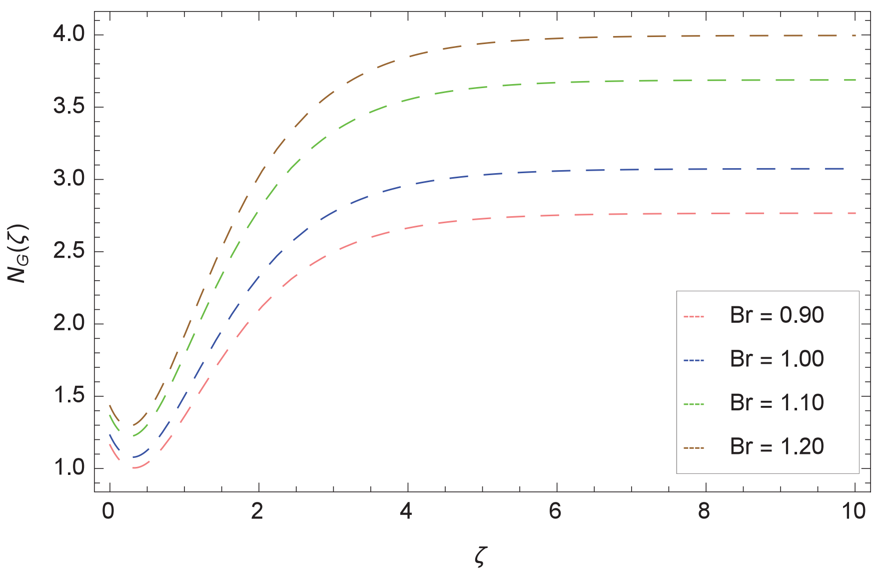

FIGURE 29 Influence of Brinkman number Br on entropy generation rate $N_G(\zeta)$

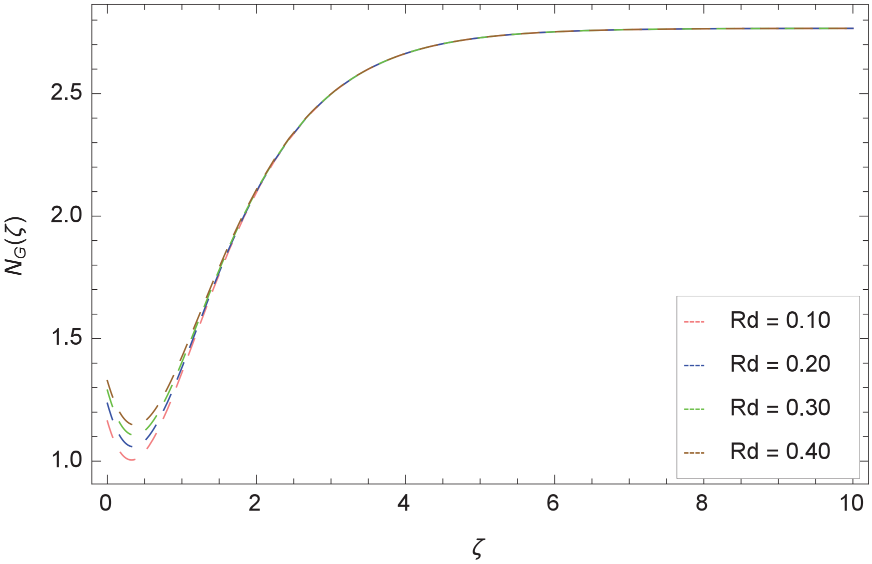

FIGURE 30 Influence of thermal radiation parameter Rd on entropy generation rate $N_G(\zeta)$

through f_w. Figure 24 is drawn to realize the effect of Prandtl number Pr on gyrotactic microorganisms concentration $\chi(\zeta)$. The gyrotactic microorganisms concentration is reduced for the rising values of Pr. The outcomes of stretching/shrinking parameter λ and gyrotactic microorganisms concentration $\chi(\zeta)$ are depicted in Figure 25, which shows that gyrotactic microorganisms concentration is minimum for the greater values of λ.

Entropy generation rate $N_G(\zeta)$ is reduced when the Casson nanofluid parameter β is increased for the higher values of β. This phenomena is clearly shown by Figure 26. The effect of Reynolds number Re on entropy generation rate is shown in Figure 27. Entropy of the system is maximum for the high values of Re. Figure 28 highlightens the effect of magnetic field parameter M on entropy generation rate $N_G(\zeta)$. It is noted that entropy generation rate approaches to its maximum value for the integral values of M. Similarly, increasing behaviors are seen in Figures 29 and 30 for the Brinkman number Br and thermal radiation parameter Rd, respectively, to show the effects on entropy generation rate $N_G(\zeta)$.

6 | CONCLUSIONS

The leading edge accretion (or ablation) problem is modeled with Cattaneo–Christov heat and mass flux in the presence of entropy generation, thermal radiation, magnetic field, and gyrotactic microorganisms. HAM is used to get the solution of the problem. Effects of all the parameters on the different profiles are provided.

ACKNOWLEDGMENTS

The authors wish to thank the referee for his comments and suggestions. The authors acknowledge the financial support provided by the Center of Excellence in Theoretical and Computational Science (TaCS-CoE), KMUTT. Moreover, this research was supported by The Science, Research and Innovation Promotion Funding (TSRI) (Grant no. FRB650070/0168). This research block grants was managed under Rajamangala University of Technology Thanyaburi (FRB65E0633M.2). The authors extend their appreciation to the Deanship of Scientific Research at King Khalid University, Abha, Saudi Arabia for funding this work through research groups program under grant number RGP.1/248/43. The first author is thankful to the Higher Education Commission (HEC) Pakistan for funding through the SRGP project No. 10534.

CONFLICT OF INTEREST

The authors declare that there is no conflict of interest.

ORCID

Noor Saeed Khan https://orcid.org/0000-0003-0991-7846
Wiyada Kumam https://orcid.org/0000-0001-8773-4821
Poom Kumam https://orcid.org/0000-0002-5463-4581

REFERENCES

[1] Bejan, A.: Second law analysis in heat transfer. Energy 5, 720–732 (1980)

[2] Sahoo, A., Nandkeolyar, R.: Entropy generation and dissipative heat transfer analysis of mixed convective hydromagnetic flow of a Casson nanofluid with thermal radiation and Hall current. Sci. Rep. 11, 3926 (2021)

[3] Abbas, S.Z., Khan, W.A., Kadry, S., Khan, M.I., Waqas, M., Khan, M.I.: Entropy optimized Darcy–Forchheimer nanofluid (Silicon dioxide, Molybdenum disulfide) subject to temperature dependent viscosity. Comp. Methods Programs Biomed. 190, 105363 (2020)

[4] Alsaadi, F.E., Hayat, T., Sohail, A.K., Alsaadi, F.E., Khan, M.I.: Investigation of physical aspects of cubic autocatalytic chemically reactive flow of second grade nanomaterial with entropy optimization. Comp. Methods Programs Biomed. 183, 105061 (2020)

[5] Khanl, I.K., Khan, A.K., Hayat, T., Khan, M.I., Alsaedi, A.: Entropy optimization analysis in MHD nanomaterials (TiO_2-GO) flow with homogeneous and heterogeneous reactions. Comp. Methods Programs Biomed. 184, 105111 (2020)

[6] Khan, N.S., Zuhra, S., Shah, Q.: Entropy generation in two phase model for simulating flow and heat transfer of carbon nanotubes between rotating stretchable disks with cubic autocatalysis chemical reaction. Appl. Nanosci. 9, 1797–1822 (2019)

[7] Khan, N.S., Shah, Q., Bhaumik, A., Kumam, P., Thounthong, P., Amiri, I.: Entropy generation in bioconvection nanofluid flow between two stretchable rotating disks. Sci. Rep. 10, 4448 (2020)

[8] Usman, A.H., Khan, N.S., Humphries, U.W., Ullah, Z., Shah, Q., Kumam, P., Thounthong, P., Khan, W., Kaewkhao, A., Bhaumik, A.: Computational optimization for the deposition of bioconvection thin Oldroyd-B nanofluid with entropy generation. Sci. Rep. 11(1), 1164 (2021)

[9] Khan, N.S., Shah, Z., Islam, S., Khan, I., Alkanhal, T.A., Tlili, I.: Entropy generation in MHD mixed convection non-Newtonian second-grade nanoliquid thin film flow through a porous medium with chemical reaction and stratification. Entropy 21, 139 (2019)

[10] Khan, N.S., Zuhra, S., Shah, Z., Bonyah, E., Khan, W., Islam, S., Khan, A.: Hall current and thermophoresis effects on magnetohydrodynamic mixed convective heat and mass transfer thin film flow. J. Phys. Commun. 3, 035009 (2019)

[11] Khan, N.S., Kumam, P., Thounthong, P.: Magnetic field promoted irreversible process of water based nanocomposites with heat and mass transfer flow. Sci. Rep. 1, 11692 (2021)

[12] Khan, N.S., Kumam, P., Thounthong, P.: Renewable energy technology for the sustainable development of thermal system with entropy measures. Int. J. Heat Mass Transf. 145, 118713 (2019)

[13] Khan, N.S., Shah, Q., Sohail, A., Kumam, P., Thounthong, P., Muhammad, T.: Mechanical aspects of Maxwell nanofluid in dynamic system with irreversible analysis. ZAMM J. Appl. Math. Mech. Z. Angewandte Math. Mech. 101, e202000212 (2021)

[14] Usman, A.H., Khan, N.S., Rano, S.A., Humphries, U.W., Kumam, P.: Computational investigations of Arrhenius activation energy and entropy generation in a viscoelastic nanofluid flow thin film sprayed on a stretching cylinder. J. Adv. Res. Fluid Mech. Therm. Sci. 86(1), 27–51 (2021)

[15] Alaidrous, A.A., Eid, M.R.: 3-D electromagnetic radiative non-Newtonian nanofluid flow with Joule heating and higher-order reactions in porous materials. Sci. Rep. 10, 14513 (2020)

[16] Shehzad, S.A., Mabood, F., Rauf, A., Izadi, M., Abbasi, F.M.: Rheological features of non-Newtonian nanofluids flows induced by stretchable rotating disk. Phys. Scr. 96, 035210 (2021)

[17] Kolsi, L., Selimefendigil, F., Said, L.B., Mesloub, A., Alresheedi, F.: Forced convection of non-Newtonian nanofluid flow over a backward facing step with simultaneous effects of using double rotating cylinders and inclined magnetic field. Mathematics 9, 3002 (2021)

[18] Ramesh, K., Ojjela, O.: Entropy generation analysis of natural convective radiative second grade nanofluid flow between parallel plates in a porous medium. Appl. Math. Mech. (Eng. Ed.) 40(4), 481–498 (2019)

[19] Yin, J., Zhang, X., Rehman, M.I.Ur., Hamid, A.: Thermal radiation aspect of bioconvection flow of magnetized Sisko nanofluid along a stretching cylinder with swimming microorganisms. Case Stud. Therm. Eng. 30, 101771 (2022)

[20] Khan, I., Rehman, K. Ur., Malik, M.Y.: Physical aspects of nanoparticles in non-Newtonian liquid in the presence of chemically reactive species through parabolic approach. Result. Phys. 7, 2540–2549 (2017)

[21] Hayat, T., Khan, M.I., Waqas, M., Alsaedi, A.: Radiative flow of hyperbolic tangent liquid subject to Joule heating. Result. Phys. 7, 2179–2203 (2017)

[22] Hamid, A., Khan, M., Alshomrani, A.S.: Non-linear radiation and chemical reaction effects on slip flow of Williamson nanofluid due to a static/moving wedge: a revised model. Appl. Nanosci. 10, 3171–3181 (2020)

[23] Muntazir, R.M.A., Mushtaq, M., Shahzadi, S., Jabeen, K.: Influence of chemically reacting ferromagnetic Carreau nanofluid over a stretched sheet with magnetic dipole and viscous dissipation. Math. Prob. Eng. 2021, 1–12 (2021)

[24] Khan, N.S.: Bioconvection in second grade nanofluid flow containing nanoparticles and gyrotactic microorganisms. Braz. J. Phys. 43, 227–241 (2018)

[25] Khan, N.S., Gul, T., Khan, M.A., Bonyah, E., Islam, S.: Mixed convection in gravity-driven thin film non-Newtonian nanofluids flow with gyrotactic microorganisms. Result. Phys. 7, 4033–4049 (2017)

[26] Khan, N.S., Gul, T., Islam, S., Khan, W.: Thermophoresis and thermal radiation with heat and mass transfer in a magnetohydrodynamic thin film second-grade fluid of variable properties past a stretching sheet. Eur. Phys. J. Plus 32, 11 (2017)

[27] Palwasha, Z., Khan, N.S., Shah, Z., Islam, S., Bonyah, E.: Study of two dimensional boundary layer thin film fluid flow with variable thermo-physical properties in three dimensions space. AIP Adv. 8, 105318 (2018)

[28] Khan, N.S., Gul, T., Islam, S., Khan, A., Shah, Z.: Brownian motion and thermophoresis effects on MHD mixed convective thin film second-grade nanofluid flow with Hall effect and heat transfer past a stretching sheet. J. Nanofluids 6, 812–829 (2017)

[29] Khan, N.S., Zuhra, S., Shah, Z., Bonyah, E., Khan, W., Islam, S.: Slip flow of Eyring–Powell nanoliquid film containing graphene nanoparticles. AIP Adv. 8, 115302 (2019)

[30] Khan, N.S., Gul, T., Kumam, P., Shah, Z., Islam, S., Khan, W., Zuhra, S., Sohail, A.: Influence of inclined magnetic field on Carreau nanoliquid thin film flow and heat transfer with graphene nanoparticles. Energies 12(8), 1459 (2019)

[31] Khan, N.S.: Study of two dimensional boundary layer flow of a thin film second grade fluid with variable thermo-physical properties in three dimensions space. Filomat 33, 5387–5405 (2019)

[32] Khan, N.S., Zuhra, S.: Boundary layer unsteady flow and heat transfer in a second grade thin film nanoliquid embedded with graphene nanoparticles past a stretching sheet. Adv. Mech. Eng. 11(11), 1–11 (2019)

[33] Usman, A.H., Khan, N.S., Humphries, U.W., Shah, Z., Kumam, P., Khan, W., Khan, A., Rano, S.A., Ullah, Z.: Development of dynamic model and analytical analysis for the diffusion of different species in non-Newtonian nanofluid swirling flow. Front. Phys. 8, 616790 (2021)

[34] Ali, B., Hussain, S., Abdal, S., Mehdi, M.M.: Impact of Stefan blowing on thermal radiation and Cattaneo–Christov characteristics for nanofluid flow containing microorganisms with ablation/accretion of leading edge: FEM approach. Eur. Phys. J. Plus 135, 821 (2020)

[35] Vasu, B., Ray, A.K., Beg, O.A., Gorla, R.S.R.: Magneto-bioconvection flow of a Casson thin film with nanoparticles over an unsteady stretching sheet: HAM and GDQ computation. Int. J. Numer. Methods Heat Fluid Flow 29(11), 427–4309 (2019)

[36] Jiang, Y., Zhang, J., Abdeljawad, T., Ahmad, S., Khan, M.N., Rehman, A., Almaliki, A.H., El-Shafay, A.S.: Blasius–Rayleigh–Stokes flow of hybrid nanomaterial liquid past a stretching surface with generalized Fourier's and Fick's law. Nanomaterials 12, 439 (2022)

[37] Ali, L., Liu, X., Ali, B.: Finite element analysis of variable viscosity impact on MHD flow and heat transfer of nanofluid using the Cattaneo–Christov model. Coatings 10, 395 (2020)

[38] Ilias, M.R., Ismail, N.S., Raji, N.H.A., Rawi, N.A., Shafie, S.: Unsteady aligned MHD boundary layer flow and heat transfer of a magnetic nanofluids past an inclined plate. Int. J. Mech. Eng. Robot. Res. 9(2), 1–10 (2020)

[39] Zeeshan, Rasheed, H. Ur., Khan, W., Khan, I., Alshammari, N., Hamadneh, N.: Numerical computation of 3D Brownian motion of thin film nanofluid flow of convective heat transfer over a stretchable rotating surface. Sci. Rep. 12, 2708 (2022)

[40] Goqo, S.P., Oloniiju, S.D., Mondal, H., Sibanda, P., Motsa, S.S.: Entropy generation in MHD radiative viscous nanofluid flow over a porous wedge using the bivariate spectral quasi-linearization method. Case Stud. Therm. Eng. 12, 774–788 (2018)

[41] Hosseinzadeh, Kh., Asadi, A., Mogharrebi, A.R., Khalesi, J., Mousavisani, S., Ganji, D.D.: Entropy generation analysis of $(CH_2OH)_2$ containing CNTs nanofluid flow under effect of MHD and thermal radiation. Case Stud. Therm. Eng. 14, 10042 (2019)

[42] Khan, N.S., Gul, T., Islam, S., Khan, I., Alqahtani, A.M., Alshomrani, A.S.: Magnetohydrodynamic nanoliquid thin film sprayed on a stretching cylinder with heat transfer. J. Appl. Sci. 7, 271 (2017)

[43] Khan, N.S., Kumam, P., Thounthong, P.: Computational approach to dynamic systems through similarity measure and homotopy analysis method for renewable energy. Crystals 10(12), 1086 (2020)

[44] Khan, N.S., Shah, Q., Sohail, A., Kaewkhao, A., Kumam, P., Zubair, S., Ullah, N., Thounthong, P.: Rotating flow assessment of magnetized mixture fluid suspended with hybrid nanoparticles and chemical reactions of species. Sci. Rep. 11(1), 11277 (2021)

[45] Zuhra, S., Khan, N.S., Khan, M.A., Islam, S., Khan, W., Bonyah, E.: Flow and heat transfer in water based liquid film fluids dispensed with graphene nanoparticles. Result. Phys. 8, 1143–1157 (2018)

[46] Khan, N.S., Usman, A.H., Sohail, A., Hussanan, A., Shah, Q., Ullah, N., Kumam, P., Thounthong, P., Humphries, U.W.: A framework for the magnetic dipole effect on the thixotropic nanofluid flow past a continuous curved stretched surface. Crystals 11, 645 (2021)

[47] Khan, N.S., Usman, A.H., Kaewkhao, A., Kumam, P., Thounthong, P., Humphries, U.W.: Exploring the nanomechanical concepts of development through recent updates in magnetically guided system. Sci. Rep. 11(1), 13576 (2021)

[48] Khan, N.S., Gul, T., Islam, S., Khan, W., Khan, I., Ali, L.: Thin film flow of a second-grade fluid in a porous medium past a stretching sheet with heat transfer. Alex. Eng. J. 57, 1019–1031 (2017)

[49] Zuhra, S., Khan, N.S., Alam, A., Islam, S., Khan, A.: Buoyancy effects on nanoliquids film flow through a porous medium with gyrotactic microorganisms and cubic autocatalysis chemical reaction. Adv. Mech. Eng. 12(1), 1–17 (2020)

[50] Palwasha, Z., Islam, S., Khan, N.S., Ayaz, H.: Non-Newtonian nanoliquids thin film flow through a porous medium with magnetotactic microorganisms. Appl. Nanosci. 8, 1523–1544 (2018)

[51] Khan, N.S.: Mixed convection in MHD second grade nanofluid flow through a porous medium containing nanoparticles and gyrotactic microorganisms with chemical reaction. Filomat 33, 4627–4653 (2019)

[52] Zuhra, S., Khan, N.S., Shah, Z., Islam, Z., Bonyah, E.: Simulation of bioconvection in the suspension of second grade nanofluid containing nanoparticles and gyrotactic microorganisms. AIP Adv. 8, 105210 (2018)

[53] Zuhra, S., Khan, N.S., Islam, S.: Magnetohydrodynamic second grade nanofluid flow containing nanoparticles and gyrotactic microorganisms. Comput. Appl. Math. 37, 6332–6358 (2018)

[54] Zahra, A., Mahanthesh, B., Basir, M.F.M., Imtiaz, M., Mackolil, J., Khan, N.S., Nabwey, H.A., Tlili, I.: Mixed radiated magneto Casson fluid flow with Arrhenius activation energy and Newtonian heating effects: flow and sensitivity analysis. Alex. Eng. J. 57, 1019–1031 (2020)

[55] Liaqat, A., Asifa, T., Ali, R., Islam, S., Gul, T., Kumam, P., Mukhtar, S., Khan, N.S., Thounthong, P.: A new analytical approach for the research of thin-film flow of magneto hydrodynamic fluid in the presence of thermal conductivity and variable viscosity. ZAMM J. Appl. Math. Mech. Z. Angewandte Math. Mech. 101(2), e201900292 (2020)

[56] Khan, N.S., Kumam, P., Thounthong, P.: Second law analysis with effects of Arrhenius activation energy and binary chemical reaction on nanofluid flow. Sci. Rep. 10, 1226 (2020)

[57] Khan, N.S., Shah, Q., Sohail, A.: Dynamics with Cattaneo–Christov heat and mass flux theory of bioconvection Oldroyd-B nanofluid. Adv. Mech. Eng. 12(8), 1–20 (2020)

[58] Shijun, L.: On the homotopy analysis method for non-linear problems. Appl. Math. Comput. 147, 499–513 (2004)

[59] Liaqat, A., Khan, N.S., Ali, R., Islam, S., Kumam, P., Thounthong, P.: Novel insights through the computational techniques in unsteady MHD second grade fluid dynamics with oscillatory boundary conditions. Heat Transf. 50(3), 2502–2524 (2020)

[60] Khan, N.S., Shah, Q., Sohail, A., Kumam, P., Thounthong, P., Bhaumik, A., Ullah, Z.: Lorentz forces effects on the interactions of nanoparticles in emerging mechanisms with innovative approach. Symmetry 12(10), 1700 (2020)

[61] Zuhra, S., Khan, N.S., Islam, S., Nawaz, R.: Complexiton solutions for complex KdV equation by optimal homotopy asymptotic method. Filomat 33(19), 6195–6211 (2020)

[62] Khan, N.S., Ali, L., Ali, R., Kumam, P., Thounthong, P.: A novel algorithm for the computation of systems containing different types of integral and integro-differential equations. Heat Transf. 50(4), 3065–3078 (2020)

[63] Usman, A.H., Khan, N.S., Rano, S.A., Maitama, M., Humphries, U.W.: Study of heat and mass transfer in MHD flow of sutterby ferrofluid over a curved stretching surface with magnetic dipole and chemical reaction effect. Thai J. Math. 19(3), 1037–1055 (2021)

[64] Ramzan, M., Khan, N.S., Kumam, P., Khan, R.: A numerical study of chemical reaction in a nanofluid flow due to rotating disk in the presence of magnetic field. Sci. Rep. 11(1), 19399 (2021)

[65] Ramzan, M., Khan, N.S., Kumam, P.: Mechanical analysis of non-Newtonian nanofluid past a thin needle with dipole effect and entropic characteristics. Sci. Rep. 11(1), 19378 (2021)

[66] Khan, N.S., Humphries, U.W., Kumam, W., Kumam, P., Muhammad, T.: Bioconvection Casson nanoliquid film sprayed on a stretching cylinder in the portfolio of homogeneous-heterogeneous chemical reactions. ZAMM J. Appl. Math. Mech. Z. Angewandte Math. Mech. 102, e202000222 (2022)

How to cite this article: Khan, N.S., Humphries, U.W., Kumam, W., Kumam, P., Muhammad, T.: Assessment of irreversibility optimization in Casson nanofluid flow with leading edge accretion or ablation. Z. Angew. Math. Mech. 102, e202000207 (2022). https://doi.org/10.1002/zamm.202000207